New metric for IQ imbalance compensation in optical QPSK coherent systems

Trung Hien Nguyen, Pascal Scalart, Mathilde Gay, Laurent Bramerie,
Christophe Peucheret, Fausto Gomez Agis, Olivier Sentieys, Jean-Claude
Simon, Michel Joindot

HAL Id: hal-01941892
https://inria.hal.science/hal-01941892

New Metric for IQ Imbalance Compensation in Optical QPSK Coherent Systems

Trung-Hien Nguyen,[*][†]
Pascal Scalart,[‡]
Mathilde Gay,
Laurent Bramerie,
Christophe Peucheret,
Fausto Gomez-Agis,[§]
Olivier Sentieys,
Jean-Claude Simon and
Michel Joindot

Abstract

We report on a simple alternative method for the compensation of quadrature imbalance in optical quadrature phase-shift-keying (QPSK) coherent systems. By introducing a new metric, the phase imbalance can be determined and compensated. The proposed method is theoretically and numerically analyzed. In particular, it is shown that the method exhibits a small bias of estimated phase imbalance value. Thanks to its deterministic property, this bias can be simply compensated by incorporating at the receiver a phase rotator (or phase shift) whose value can be determined based on an analytical analysis. Moreover, the algorithm is also experimentally validated through bit-error-rate (BER) and error vector magnitude (EVM) measurements. A good agreement on the performance of the proposed method with that of the Gram-Schmidt orthogonalization procedure (GSOP) is shown in a 20 Gbit/s optical QPSK experiment. The robustness of both methods was verified with up to 30° phase imbalance by comparing the signal with and without phase imbalance compensation. A 10% reduction of EVM is achieved with our method for a high phase imbalance of 30° while the implementation complexity can be reduced owing to the suppression of the use of square-root operators.
Keywords: Coherent communications, Fiber optical communications, IQ imbalance, Modulation.

1 Introduction

Optical transmission systems using polarization division-multiplexed quadrature phase-shift-keying (PDM-QPSK) and coherent detection at 100 Gbit/s have been the object of intensive investigations and are already commercialized. One of the aims of the optical fiber communication industry is now to move towards systems carrying over 100 Gbit/s per wavelength channel [1]. This trend towards always increasing capacities has activated a renewed interest

---

[*]T.-H. Nguyen, M. Gay, L. Bramerie, C. Peucheret, F. Gomez-Agis, J.-C. Simon, M. Joindot are with FOTON Laboratory, CNRS, University of Rennes 1, ENSSAT, Lannion, France.

[†]T.-H. Nguyen is now with the OPERA department, Université Libre de Bruxelles, Brussels, Belgium.

[‡]P. Scalart, O. Sentieys are with INRIA, IRISA, University of Rennes 1, Campus de Beaulieu, Rennes, France.

[§]F. Gomez-Agis is now with Dept. of Electrical Engineering, Technische Universiteit Eindhoven, Eindhoven, Netherlands.

in coherent optical communication systems thanks to their improved receiver sensitivity and spectral efficiency, and ability to mitigate transmission impairments in the digital domain [2].

As in in-phase/quadrature (I/Q) down-conversion radio architectures [3], the I and Q components of the optical field should be ideally orthogonal to each other in an optical QPSK coherent system. However, hardware implementation imperfections and finite tolerances of the front-end components, such as incorrect bias-point settings in the modulator, imperfect splitting ratio of couplers, photodiodes responsivities mismatch and incorrect adjustment of polarization splitters can create amplitude and phase imbalance, known as quadrature imbalance (or IQ imbalance), which destroys the orthogonality between components of the received signal [4].

Since digital signal processing (DSP) circuits are becoming increasingly faster, providing simple and efficient compensation of linear [5] and, possibly, non-linear [6] impairments, it is important to assess their potential for the compensation of this detrimental loss of orthogonality in the receiver. Some effort has been dedicated to the compensation of IQ imbalance with the help of DSP. IQ imbalance causing inter-carrier interference (ICI) due to imperfect image rejection in multicarrier direct-detection systems has been analytically and numerically investigated [3], and extended to deal with frequency-dependent IQ imbalance [7]. In multicarrier coherent-detection systems, several frequency domain compensation methods for IQ imbalance have been reported, both for wireless and optical transmission. Those include joint transmitter (Tx) and receiver (Rx) IQ imbalance compensation [8]-[9] for the blind compensation class (in the sense that no known training symbols are required), the pilot-assisted method [10], the use of a novel training symbol structure [11], or the joint compensation of phase noise and IQ imbalance [12]. For single carrier optical coherent detection systems, some work exploiting time-domain compensation has been numerically and experimentally carried out. More specifically, IQ imbalance has been corrected in optical coherent QPSK systems by applying different methods such as the Gram-Schmidt orthogonalization procedure (GSOP) [13], the ellipse correction method (EC) [14], and IQ compensation based on the constant modulus algorithm (CMA) [15] or the statistical properties of received signals [16].

In this paper, we comprehensively investigate an alternative method for IQ imbalance compensation [17] based on the definition and computation of a suitable novel metric for the detected signal, in order to estimate and compensate for the phase imbalance. The approach using this new metric, called best-matched signal estimation method (MSEM), provides an interesting alternative to existing algorithms thanks to its reduced complexity and a comparable performance. More particularly, our main contributions in this paper are: (i) a comprehensive analytical analysis of the proposed IQ imbalance compensation method; (ii) numerical validation of the derived analytical expression in the presence of additive noise; (iii) finding and numerically proving the existence of a small deterministic bias of the estimated phase imbalance. These new contributions strongly confirm our experimental results of the proposed IQ imbalance compensation method. Moreover, the proposed method requires no square-root operators, which can make its implementation in hardware platforms simpler. Furthermore, our method provides information on the phase imbalance value between I and Q components, which can be helpful for the characterization and calibration of the IQ modulator or the coherent receiver. The accuracy of our method is compared to that of the GSOP approach by evaluating the bit-error-rate (BER) and the error vector magnitude (EVM) of compensated constellations. The performance of the proposed MSEM method matches that of the GSOP, while its implementation complexity is reduced.

This paper is organized as follows: Section 2 presents in details an analytical analysis of the proposed method for IQ imbalance compensation based on the introduction of a new metric. Numerical simulations of the proposed method are carried out in Section 3 to demonstrate the effectiveness of the method. Section 4 describes the experimental setup used to validate this
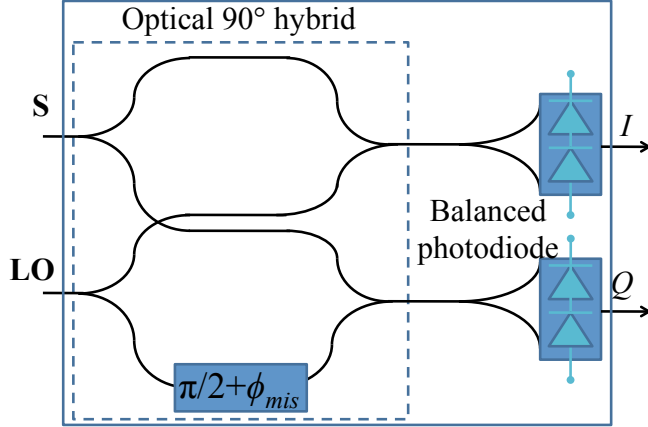
Figure 1: Structure of the coherent receiver, including a 90° hybrid, in the presence of the phase imbalance (or mismatch) ϕ_{mis}. S: signal input, LO: local oscillator input.

work, along with a discussion of the achieved results in Section 5. Finally, conclusions are drawn in Section 6.

2   Analytical analysis

In our study, we focus only on phase imbalance since amplitude imbalance can be corrected at the hardware level (for instance thanks to the use of automatic gain controlled trans-impedance amplifiers) [18]. More specifically, the correction of phase imbalance introduced at the receiver is investigated with the assumption of perfect orthogonality between the I and Q components in the transmitted signals. In order to demonstrate how the maximization of a proposed metric can lead to IQ imbalance compensation, we first define and derive an analytical expression for such a new parameter for a QPSK signal. Without loss of generality, the QPSK signal at the transmitter is assumed to have unit power. ϕ_S is the information carrying phase, which takes four possible values $(2k+1) \cdot \pi/4$, $k = 0, 1, 2, 3$ with the same probability. During transmission over an optical channel, this signal is corrupted by amplified spontaneous emission (ASE) noise, whose complex envelope $n = n_C + j \cdot n_S$ can be modeled as additive white Gaussian noise (AWGN). The QPSK signal is then detected by mixing with a local oscillator in a coherent receiver made from an optical 90° hybrid and a pair of balanced photodiodes to extract the in-phase (I) and quadrature (Q) components, as illustrated in Fig. 1. The resulting two baseband electrical components are obtained by the sum of quadratic detection in balanced photodiodes. To simplify our analysis, the carrier frequency offset (CFO) between the transmitter and receiver lasers is assumed to be zero, other noise sources (i.e. shot noise, thermal noise) are assumed to be negligible, and the power of the received samples is normalized to one. We can then express the I and Q terms by the following equations

$$I \propto \mathrm{Re}\left\{E_S E_{LO}^*\right\}, \tag{1}$$

$$Q \propto \mathrm{Im}\left\{E_S E_{LO}^* . \mathrm{e}^{j\phi_{mis}}\right\}, \tag{2}$$

where E_S and E_{LO} represent the fields of the signal (S) and local oscillator (LO) at the inputs of the 90° hybrid in the receiver, Re and Im denote the real and imaginary parts of the beating products between the S and LO, respectively. ϕ_{mis} represents the phase imbalance (or mismatch) stemming from phase misalignment between the two branches created in the coherent

3

receiver. This term cancels for an ideal optical 90∘ hybrid. It is noted that imperfections in the implementation of the QPSK modulator could also lead to $\phi_{mis} \neq 0$ and consequently to a loss of orthogonality. However, the focus of the present analysis is on phase imbalance at the receiver and ϕ_{mis} lies in the range $[-90°, 90°]$.

The I and Q components can be expressed by equations (1) and (2) as follows

$$\begin{cases} I = \cos \phi_S + n_C \\ Q = \sin (\phi_S + \phi_{mis}) + n_C \sin \phi_{mis} + n_S \cos \phi_{mis} \end{cases}, \tag{3}$$

where n_C and n_S are zero mean random Gaussian variables with the same variance σ^2 that are furthermore assumed to be uncorrelated. The MSEM method consists in applying a phase shift, ϕ_{var}, to the received signal, $R = I + j \cdot Q$, to form a new quantity $Q_n = \text{Im} \left\{ R \cdot e^{j \cdot \phi_{var}} \right\}$ and consider it as a new quadrature component. A new metric, D, is introduced and defined according to

$$D = \frac{\mathbf{E}^2 \left(|r|^2 \right)}{\sigma_{|r|^2}^2}, \tag{4}$$

where $\mathbf{E}(\cdot)$ and $|\cdot|$ are the mean and modulus operators, respectively. $\sigma_{|r|^2}^2$ represents the variance of the squared modulus of the modified signal, $r = I + j \cdot Q_n$. This new metric is similar to the use of high-order statistics of circular signals to solve the source separation problem [19]. Although higher ($\geq$ 4th)-order statistics of the signal can be utilized [19], only second-order statistics are used in our case to keep a reasonable complexity while providing an acceptable estimation accuracy.

After some mathematical manipulation, Q_n can be written as

$$\begin{aligned} Q_n = & \cos \phi_S \cdot \sin \phi_{var} + \sin (\phi_S + \phi_{mis}) \cdot \cos \phi_{var} + n_C \cdot \sin \phi_{var} \\ & + (n_C \sin \phi_{mis} + n_S \cos \phi_{mis}) \cdot \cos \phi_{var}. \end{aligned} \tag{5}$$

To simplify the calculations, the following quantities are defined

$$\begin{cases} \alpha = \sin \phi_{var} + \sin \phi_{mis} \cdot \cos \phi_{var} \\ \beta = \cos \phi_{mis} \cdot \cos \phi_{var} \end{cases}. \tag{6}$$

The expected value of $|r|^2$ (calculated in Appendix 6) is derived as

$$\mathbf{E} \left(|r|^2 \right) = \left(\frac{1}{2} + \sigma^2 \right) \cdot \left(1 + \alpha^2 + \beta^2 \right). \tag{7}$$

The variance of $|r|^2$ is given by (Appendix 6)

$$\sigma_{|r|^2}^2 = \alpha^2 \beta^2 + 2 \left(1 + 2\alpha^2 + \left(\alpha^2 + \beta^2 \right)^2 \right) \cdot \left(1 + \sigma^2 \right) \cdot \sigma^2. \tag{8}$$

Finally, by substituting (7) and (8) into (3), the following expression of D can be found

$$D = \frac{\left(\frac{1}{2} + \sigma^2 \right)^2 \cdot \left(1 + \alpha^2 + \beta^2 \right)^2}{\alpha^2 \beta^2 + 2 \left(1 + 2\alpha^2 + \left(\alpha^2 + \beta^2 \right)^2 \right) \cdot \left(1 + \sigma^2 \right) \cdot \sigma^2}. \tag{9}$$

In the noiseless case ($\sigma^2 = 0$), introducing the expressions of α and β, given by (6), the proposed D metric without (wo) noise impact, $D_{(wo)}$ is given by

$$D_{(wo)} = \left(\frac{1 + \sin \phi_{var} \cdot \cos \phi_{var} \cdot \sin \phi_{mis}}{\cos \phi_{mis} \cdot \cos \phi_{var} \cdot (\sin \phi_{var} + \sin \phi_{mis} \cdot \cos \phi_{var})} \right)^2. \tag{10}$$
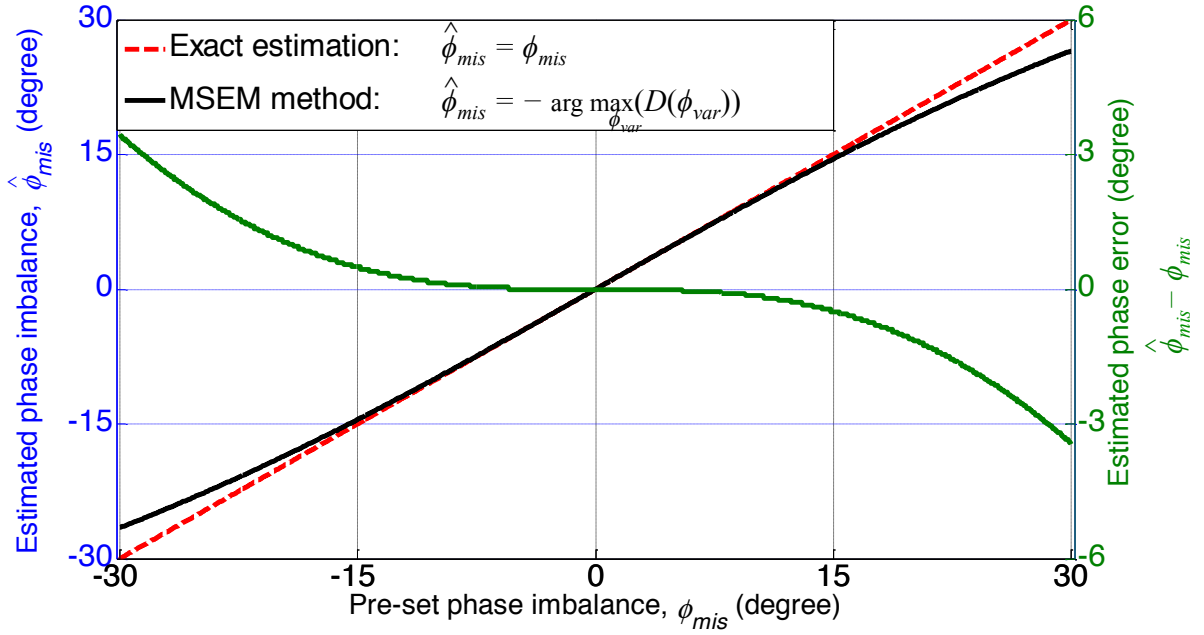
4

Figure 2: Analytical prediction of the estimated phase imbalance values, $\hat{\phi}_{mis}$ for different pre-defined phase imbalance values, ϕ_{mis} using the proposed MSEM method and their corresponding estimated phase errors, $\hat{\phi}_{mis} - \phi_{mis}$. ϕ_{var} is the IQ compensation phase value in the range $[-30°, 30°]$.

An analysis of Eq. (10) shows that $D_{(wo)}$ versus ϕ_{var} exhibits several maxima. In practical implementations, the IQ imbalance due to receiver imperfections should be sufficiently well controlled to remain in the range $[-30°, 30°]$. In this range, $D_{(wo)}$ exhibits only one maximum corresponding to $(\sin\phi_{var} + \sin\phi_{mis} \cdot \cos\phi_{var}) = 0$ or $\sin\phi_{mis} = -\tan\phi_{var}$. When the phase imbalance is small, ϕ_{var} is close to $-\phi_{mis}$.

Based on this observation, the MSEM method therefore relies on introducing a new parameter ϕ_{var} in the received signal, and the value of ϕ_{var} which maximizes D (Eq. (3)), will provide an estimator $\hat{\phi}_{mis}$ of the opposite of the phase imbalance value, or in other words, $\hat{\phi}_{mis} = -\arg\max_{\phi_{var}}(D(\phi_{var}))$. By correcting the received signal with the estimated value of the phase imbalance $\hat{\phi}_{mis}$, the IQ imbalance can be compensated for. The following paragraph will be devoted to the accuracy evaluation of the proposed algorithm.

Fig. 2 depicts the evolution of the estimated phase imbalance based on the MSEM method as a function of a predefined phase imbalance in the noiseless case. A slight deviation of the estimated phase imbalance compared to the actual one is observed, especially when the absolute value of the phase imbalance exceeds $15°$. Below this value, this estimation error is negligible. The estimated phase imbalance error is only $3.5°$ for a phase imbalance of $\pm 30°$. Note that, due to the deterministic nature of the bias introduced by the algorithm at high phase imbalance values, we can correct this issue by simply adding a specific value based on the analytical results. The proposed estimator and its bias are further studied in the presence of noise in the following section.
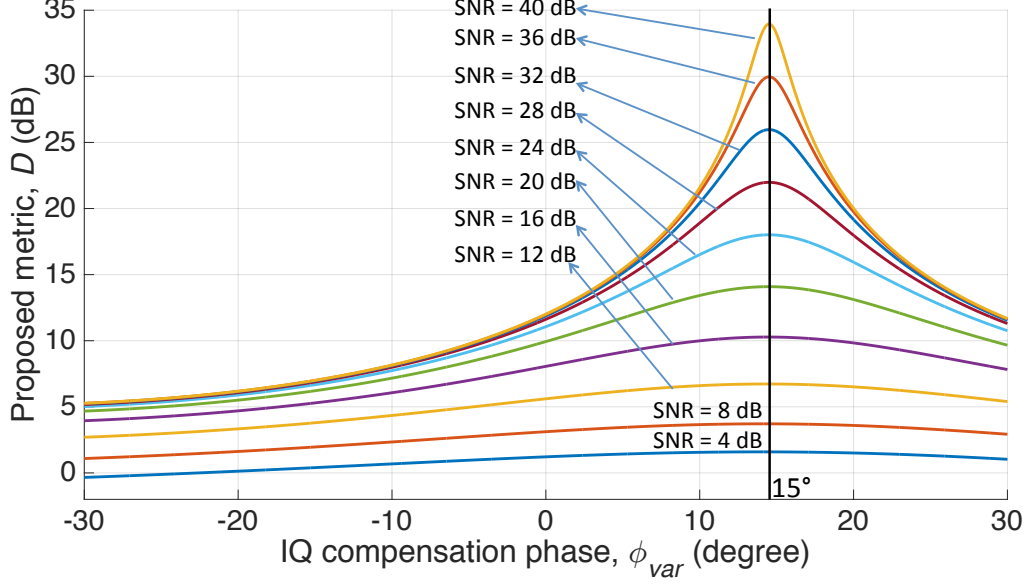
Figure 3: Calculation of the proposed metric, D, as a function of the variable IQ compensation phase ϕ_{var} for a pre-set phase imbalance of $-15°$ and different received samples SNR values.

3 Numerical simulation

In the presence of noise ($\sigma^2 \neq 0$), the derivation of an analytical expression for D is rather complex. Hence, the corresponding exact expression of the IQ compensation phase term that maximizes D is also complicated. Actually, if ϕ_0 is a phase value that maximizes $D_{(wo)}$ according to Eq. (10), it is shown in Appendix 6 that the first derivative of $D(\phi)$ at $\phi = \phi_0$ is not equal to 0 in the presence of noise. As a consequence, the maximum value of D and the corresponding estimated phase imbalance may be dependent on the SNR of the input received samples.

For this reason, we numerically study the proposed method based on Eq. (9). To this aim, the phase imbalance, ϕ_{mis}, is set to $-15°$ and assumed to be unknown at the receiver. Because the phase imbalance in optical coherent detection was assumed to be within the range $[-30°, 30°]$, the IQ compensation phase value, ϕ_{var}, used to estimate the phase imbalance is also varied within this range. The amplitude noise is represented by its variance, σ^2, in Eq. (9). Considering the unit power of the received signal, the signal SNR can be directly linked to σ^2. As a consequence, we can calculate the evolution of D as a function of the IQ compensation phase, ϕ_{var}, according to Eq. (9) for different SNR values, as shown in Fig. 3. Even though the noise level is varied, the evolution of D still exhibits one extremum in the considered range of $[-30°, 30°]$, similarly to the previous result in the absence of noise. Particularly, it is seen that the maximum values of D fall close to the opposite value of the preset phase imbalance of $-15°$. Even in the presence of a high level of noise (SNR = 4 dB), the maximum value of D still occurs at an IQ compensation phase value, of about $15°$, which is close to the opposite value of the phase imbalance, $-\phi_{mis}$, confirming the proposed criterion for IQ phase imbalance estimation is still effective in the presence of high noise levels. It should be noted that the received samples SNR values are varied from 4 dB to 40 dB, in which the smallest SNR value is chosen corresponding to the theoretical BER of about 10^{-2} of the QPSK signal [20], which corresponds to the forward-error coding (FEC) threshold assuming 28% overhead [21].

The robustness of the proposed algorithm in the presence of noise is further investigated with different predefined phase imbalances, ϕ_{mis}. Fig. 4 presents the estimated phase imbalance,
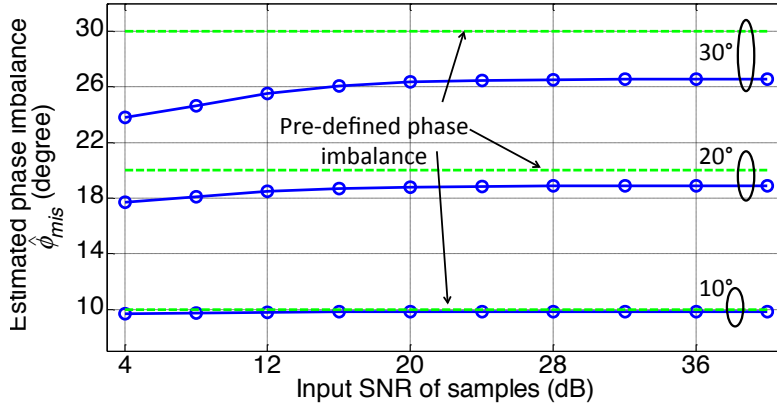
Figure 4: Estimated phase imbalance under the impact of AWGN. Dashed lines: pre-defined phase imbalances of 10°, 20° and 30°. Solid lines: estimated phase imbalance values.

$\hat{\phi}_{mis}$, as a function of the input received samples SNR for three predefined phase imbalance values of 10°, 20° and 30°. It can be observed that the estimated phase imbalance exhibits an asymptotical limit as the input SNR increases. At 10° phase imbalance, the impact of the input SNR on the proposed algorithm is negligible, resulting in no estimation error of the phase imbalance value. As the phase imbalance increases to 20°, an input SNR of 16 dB is required to reach the asymptotical limit, whose value is about 1.1° away from the pre-defined phase imbalance. This value agrees well with the theoretically calculated bias of the MSEM estimator at 20° phase imbalance, in the absence of noise (Fig. 2). Note that, the difference between the estimated phase imbalance at low input SNR (i.e. 4 dB) and that at high input SNR (i.e. 20 dB) is small (about 1°). For a phase imbalance of 30° (which is the maximum considered value), up to 20 dB input SNR is needed to achieve the asymptotical limit level. In this case, a 3.4° difference between the asymptotical limit and the pre-defined phase imbalance matches the predicted bias in the theoretical calculation (Fig. 2). For this high phase imbalance, the predicted phase imbalance at the smallest considered SNR of 4 dB is about 2.5° different from the asymptotical limit.

The numerical calculation in the presence of noise confirms again the effectiveness of the proposed MSEM estimator. More specifically, the IQ compensation phase, ϕ_{var}, resulting in the maximum value of D always happens around the opposite value of the predefined phase imbalance, ϕ_{mis}, confirming the validity of the criterion used for phase imbalance estimation (i.e. $\hat{\phi}_{mis} = -\phi_{var}$ in which ϕ_{var} maximizes D). Even though this estimator exhibits an estimation error, thanks to the deterministic nature of the algorithm bias at high phase imbalance values, this issue can be corrected by simply adding a specific value based on the analytical results (as mentioned in the previous section). This correction can be perfect for high SNR values (> 16 dB), regardless of the phase imbalance value in the range [−30°, 30°]. For low SNR values (≤ 16 dB), the correction is still valid with a negligible error, provided that the absolute phase imbalance value is less than 15°. When the absolute value of phase imbalance is superior to 15°, the bias correction introduces an estimation error smaller than 2.5°. In practice, a lookup table would be used to apply a correcting value for each phase imbalance estimation.

The proposed method will be experimentally validated in the following section. The proposed algorithm is also compared to the Gram-Schmidt orthogonalization procedure with a 20 Gbaud QPSK signal.
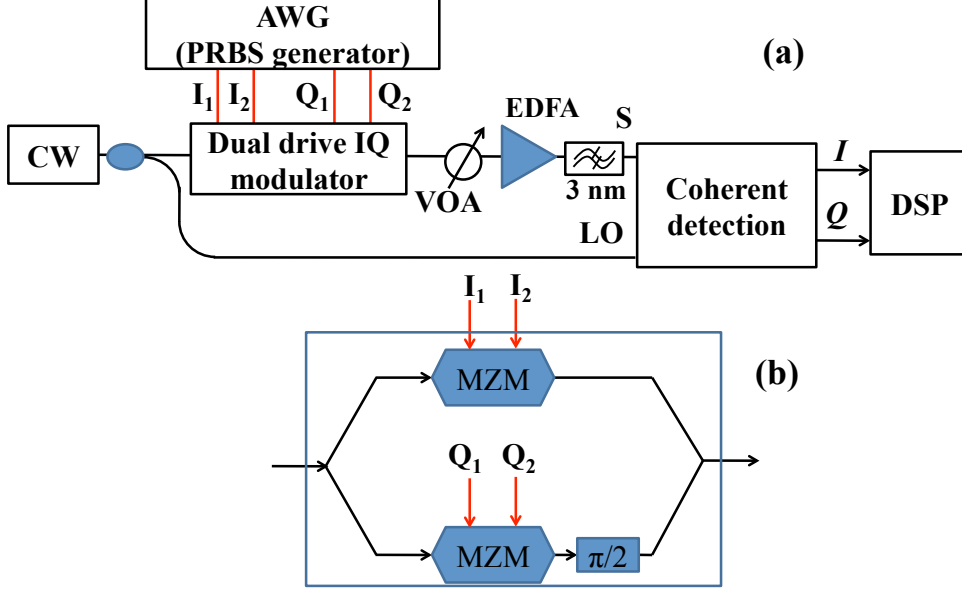
Figure 5: (a) Experimental setup for characterizing the quadrature imbalance compensation in a QPSK coherent system. (b) Dual drive IQ modulator structure. CW: continuous wave laser. AWG: arbitrary waveform generator. VOA: variable optical attenuator. EDFA: erbium-doped fiber amplifier. S: signal. LO: local oscillator. MZM: Mach-Zehnder modulator.

4 Experimental setup

The impact of non-orthogonality between the I and Q components of an optical QPSK signal is then experimentally investigated using the coherent detection system shown in Fig. 5. To simplify the setup and avoid any impact from other functionalities implemented in the digital signal processing (DSP), only one polarization and back-to-back configuration are considered in this experiment. However, it is possible to extend the implementation to a polarization diversity receiver. The laser used at the transmitter side also acts as LO at the receiver side in order to ease the carrier frequency offset compensation. The estimated linewidth of this optical source tuned at a wavelength of 1540 nm is about 100 kHz. Two pseudo-random binary sequences (PRBSs) with lengths of $2^{15} - 1$ and $2^{23} - 1$ are used as inputs to an IQ modulator, resulting in a 10 Gbaud non return-to-zero (NRZ)QPSK signal at the modulator output. The bit sequences are synthesized using arbitrary waveform generators (AWG). The use of a variable optical attenuator (VOA) followed by an erbium-doped fiber amplifier (EDFA) and a 3 nm optical bandpass filter (OBPF) allows the adjustment of the optical signal-to-noise ratio (OSNR). At the receiver side, an optical 90° hybrid (100 Gbit/s DP-QPSK integrated receiver) combines the QPSK signal and the LO. Two pairs of balanced photodiodes with a bandwidth of 32 GHz enable to retrieve the in-phase and quadrature components of the signal. Finally, the electrical signals samples are acquired by a real time oscilloscope with an electrical bandwidth of 16 GHz and sampling rate of 20 GS/s.

The phase shift of the hybrid circuit in the coherent receiver cannot be varied away from 90°. Based on the recommendations of the Optical Internetworking Forum (OIF) [22], the absolute phase imbalance value of 90° hybrid circuits should be less than 5°. Such a value is supposed to have a negligible impact in our study. In order to investigate the proposed algorithm, we therefore introduce an adjustable phase imbalance at the IQ modulator by easily tuning the voltage applied to the phase-shifter controlling the relative phase between the two arms of the
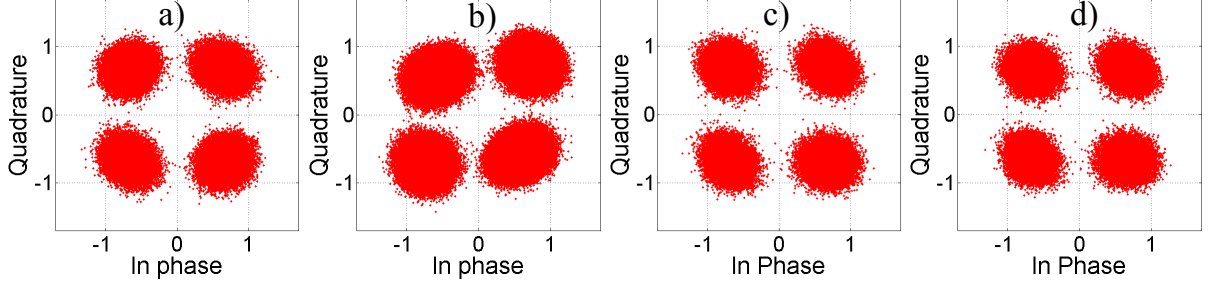
Figure 6: Experimental QPSK constellations at 12 dB OSNR: (a) without IQ imbalance, (b) with IQ imbalance of 15°, (c) recovered using the GSOP method, (d) recovered using the proposed MSEM method.

IQ modulator.

The post-processing is performed offline using the Matlab environment with the following steps: (i) IQ imbalance estimation and compensation with the investigated algorithms; (ii) equalization [23] to compensate for inter-symbol interference (ISI) induced by the limited bandwidth of equipments and decimation to the baud rate; (iii) laser phase noise estimation [24]; (iv) BER and EVM calculations. The algorithms for IQ imbalance compensation are applied to blocks of 10000 samples. Moreover, phase ambiguities are removed by processing the first 5000 samples to minimize the BER. Finally, the decoded bit sequence is compared to the transmitted one to determine the BER over 4 millions samples.

The popular EVM metric is utilized to evaluate the deviation of the reconstructed QPSK signal constellation compared to the reference one. As given in [25], the EVM can be expressed mathematically as

$$EVM = \sqrt{\frac{1}{N} \sum_{k=1}^{N} \left(|I_{ideal,k} - I_{measure,k}|^2 + |Q_{ideal,k} - Q_{measure,k}|^2 \right)}, \qquad (11)$$

where N is total number of measured symbols. $I_{ideal(measure),k}$ and $Q_{ideal(measure),k}$ are the normalized voltages of ideal (measured) in-phase and quadrature components, respectively, for the k-th symbol. The achieved results will be discussed further in the following section.

5 Results and discussion

Fig. 6(a) shows the experimental constellation without IQ imbalance when the signal OSNR is 12 dB (all OSNR values are specified over a 0.1 nm noise bandwidth). Fig. 6(b) represents the constellation of the degraded signal with 15° phase imbalance between the I and Q components. This signal degradation leads to detection errors, as it will be shown later. This degraded signal is processed with the same DSP procedure that deploys either the GSOP or the proposed MSEM method, resulting in the constellations in Fig. 6(c) and Fig. 6(d), respectively. The retrieved constellations are similar to the one without IQ imbalance, which illustrates the efficiency of the quadrature imbalance correction. In the following step, our method is experimentally validated by comparing its performance to that of the GSOP method in terms of BER and EVM.

Fig. 7 depicts the measured BER as a function of received OSNR in different cases. The theoretical curve for the BER of a QPSK signal without IQ imbalance is based on the analysis in [23]. The experimental measurement without IQ imbalance fits the theoretical trace within experimental errors. Next, the phase imbalance is tuned resulting in a BER degradation and
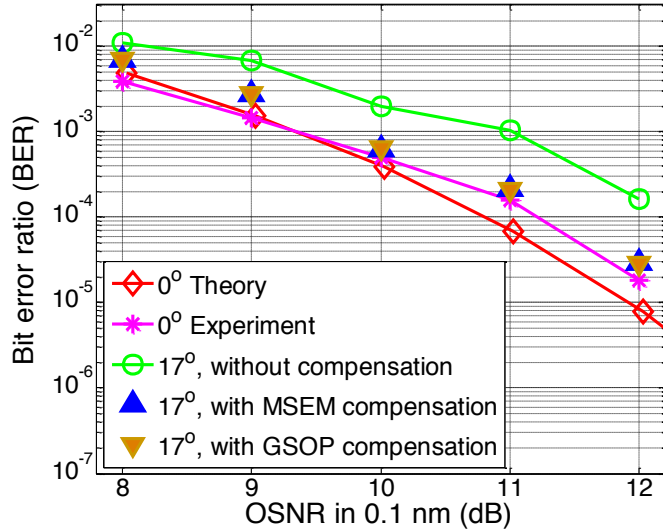
Figure 7: BER measurement as a function of OSNR (in 0.1 nm) for phase misalignments of $0°$ and $17°$ without any correction and with compensation using the GSOP and MSEM methods.

Table 1: Comparison of hardware complexity

Methods	Real-adders	Real-multipliers	Square-root operators
GSOP	$4N - 3$ [*]	$6N + 4$ [*]	2
MSEM	$(5N - 1) \cdot M$ [†]	$(4N + 5) \cdot M$ [†]	0

[*] N - total number of samples used for IQ imbalance compensation

[†] M - number of phase tests in MSEM method

an OSNR penalty of 1.7 dB at a BER of 10^{-3}. The phase imbalance is estimated at $17°$ by the algorithm. The BER curves obtained after phase imbalance compensation using the GSOP and the MSEM methods are also presented. In both cases, the IQ imbalance is well compensated, reducing the power penalty close to the experimental case without IQ imbalance. Both methods are seen to result in equivalent BER improvement.

To further investigate the accuracy of the proposed algorithm, the EVM is calculated for different phase imbalance and different OSNR values. In each case ϕ_{mis} is evaluated and the corresponding EVM is plotted in Fig. 8. Note that, the phase imbalance is estimated based on the output of the MSEM algorithm. It can be observed that, as the IQ imbalance increases, and when no compensation is applied, the EVM increases to 40% in the worst case, representing an important deviation from the optimal constellation. With both correction methods - MSEM and GSOP - and with an OSNR higher than 10 dB, the EVM remains almost constant for a phase imbalance lower than $17°$. Both methods can partially compensate for higher phase imbalances providing about 10% reduction of EVM value with the advantage of evaluating the phase imbalance in our method. Finally, for an OSNR of 8 dB, the EVM starts to increase when a phase imbalance value is superior to $9°$.

In term of hardware complexity, we qualitatively compare the required number of real adders, multipliers and square-root operators of the GSOP method with those of our proposed method, regardless of the complexity of the equalizer and other DSP blocks. It is assumed that the same total number of samples, N, is used for the different IQ imbalance compensation methods. M is the number of phase tests used in the MSEM method. Note that computing the modulus of a
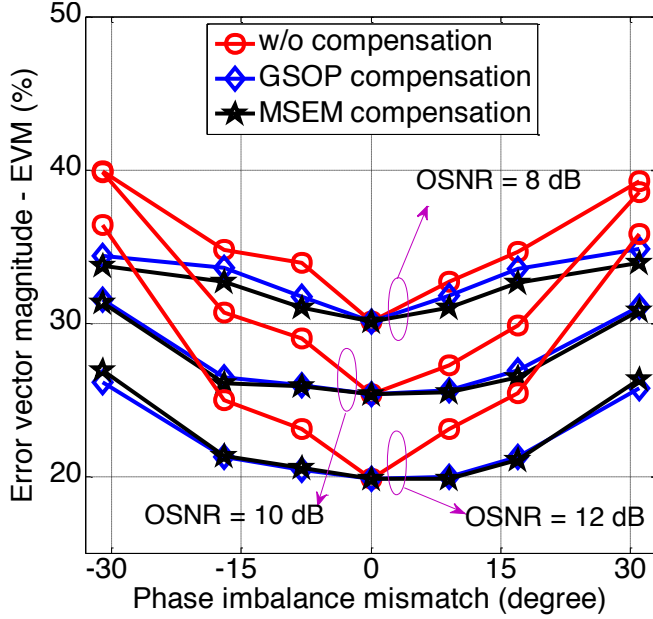
Figure 8: EVM calculation under the impact of IQ imbalance without (w/o) and with compensation by the GSOP and MSEM methods.

complex number requires 2 real multipliers and 1 real adder. Table 1 provides the summarized hardware complexities of the GSOP and MSEM methods for different operators. It can be observed that the required total number of multipliers and adders of the GSOP method is nearly M times less than that of the MSEM method due to the phase search iterations. However, the MSEM method does not require the square-root operator as for the GSOP method, bringing a potential simpler hardware implementation. It is worthy to note that the MSEM can be optimized to reduce the number of phase search iterations. In fact, based on the general equation of D (Eq. (9)), we can approximate the general form of the function $D(\phi_{var})$ as a bell shape (as illustrated in Fig. 3). By using this approximation, the maximum D value and its corresponding ϕ_{var} can be estimated with only 3 phase test values. The total number of adder and multiplier operators of the MSEM method would in this case be about 3-time larger than that of the GSOP method. A detailed optimization of the MSEM method is out of the scope of this paper.

As far as optical coherent m-QAM (i.e. 16-QAM) systems are concerned, the MSEM method may be adapted by cascading an extra step, called QPSK partitioning, as reported in [26]. By applying this technique, we only need to consider the outermost selected constellation points, which are similar to a QPSK constellation, to estimate the IQ phase imbalance. However, the MSEM may require more samples than the GSOP to maintain comparable performance, owing to the use of only outermost constellation points. This extension is also outside the scope of this paper and its implementation is straightforward. Note that, the GSOP method is also applicable for m-QAM signal constellations, for instance in [27]. In the transmission context where the impact of chromatic dispersion (CD) may impact the algorithms' performance, it is foreseen that the performance of our proposed algorithm will be similar to that of the GSOP, since both algorithms are based on the statistical properties of the received signal. A detailed study is left for future works.

11

6   Conclusion

We have proposed and demonstrated the MSEM method as an alternative solution for quadrature imbalance compensation in QPSK systems. An analytical form of a relevant new metric used to estimate quadrature imbalance has been derived. For phase imbalance superior to $15°$, the method presents an estimated phase imbalance deterministic bias which can be fully removed regardless of the value of the phase imbalance provided it is within the range $[-30°, 30°]$. The accuracy of this method is also experimentally validated by comparing it with the GSOP method by means of BER and EVM measurements. The new compensation method provides a good correction with a potential reduced implementation complexity, even when the phase imbalance reaches values as high as $30°$.

Acknowledgements

Appendix A

Based on the definition of the new metric in (4), the squared modulus of r can be written by

$$|r|^2 = (U + X)^2 + (V + Y)^2, \tag{A.1}$$

in which the variables U, X, V and Y are defined by

$$
\begin{cases}
U = \cos \phi_S \\
V = \alpha \cdot \cos \phi_S + \beta \cdot \sin \phi_S \\
X = n_C \\
Y = \alpha \cdot n_C + \beta \cdot n_S \\
\alpha = \sin \phi_{var} + \sin \phi_{mis} \cdot \cos \phi_{var} \\
\beta = \cos \phi_{mis} \cdot \cos \phi_{var}
\end{cases}
. \tag{A.2}
$$

We first calculate the expected value of $|r|^2$. From (A.1), the expectation of $\underline{r^2}$ is calculated as follows

$$
\mathbf{E}\left\{(U + X)^2 + (V + Y)^2\right\} = \mathbf{E}\left\{(U^2 + V^2)\right\} + \mathbf{E}\left\{(X^2 + Y^2)\right\} \\
+ 2\mathbf{E}(UX) + 2\mathbf{E}(VY). \tag{A.3}
$$

It must be noted that the expected value of U, V, X and Y is zero. On the other hand, U and X, V and Y are uncorrelated so that the last two terms of (A.3) are equal to 0. Moreover, ϕ_S is uniformly distributed over the four values $(2k+1) \cdot \pi/4$, $k = 0, 1, 2, 3$. Using the quantities defined in (A.2), the variances of U, V and their co-variance can be retrieved as

$$\mathbf{E}(U^2) = \frac{1}{2}, \quad \mathbf{E}(V^2) = \frac{1}{2}(\alpha^2 + \beta^2), \quad \mathbf{E}(UV) = \frac{\alpha}{2}. \tag{A.4}$$

As mentioned, n_C and n_S are random Gaussian variables with the same variance σ^2. The variances of X, Y and their covariance are

$$\mathbf{E}(X^2) = \sigma^2, \quad \mathbf{E}(Y^2) = \sigma^2(\alpha^2 + \beta^2), \quad \mathbf{E}(XY) = \alpha\sigma^2. \tag{A.5}$$

Finally, the expected value of $|r|^2$ is derived by (as in Eq. (7))

$$\mathbf{E}\left(|r|^2\right) = \left(\frac{1}{2} + \sigma^2\right) \cdot \left(1 + \alpha^2 + \beta^2\right). \tag{A.6}$$

The following part is the derivation of the variance of $|r|^2$. The variance of $|r|^2$ can be written as

$$\mathbf{Var}\left(|r|^2\right) = \mathbf{E}\left(|r|^4\right) - \left[\mathbf{E}\left(|r|^2\right)\right]^2. \tag{A.7}$$

Due to the assumption of central and uncorrelated variables, some terms cancel and the expectation of $|r|^4$ can be written as

$$\mathbf{E}\left(|r|^4\right) = \mathbf{E}\left[(U^2 + V^2)^2\right] + \mathbf{E}\left[(X^2 + Y^2)^2\right]$$
$$+ 2\mathbf{E}\left[(U^2 + V^2) \cdot (X^2 + Y^2)\right] + 4\mathbf{E}\left[(UX + VY)^2\right]. \tag{A.8}$$

Based on the definition of the QPSK signal, $(U^2 + V^2)$ is a random discrete variable taking on two equiprobable values, $1/2 \cdot (1 + (\alpha + \beta)^2)$ and $1/2 \cdot (1 + (\alpha\beta)^2)$. The first term of (A.8) can then be derived as

$$\mathbf{E}\left[(U^2 + V^2)^2\right] = \frac{1}{4}\left[\left(1 + \alpha^2 + \beta^2\right)^2 + 4\alpha^2\beta^2\right]. \tag{A.9}$$

The second term of (A.8) is calculated using the fact that all the moments of a zero mean Gaussian variable can be derived from its variance [28]. More specifically, the fourth order moments of (X, Y) can be written as

$$\begin{cases} \mathbf{E}\left[X^4\right] = 3\sigma^4 \\ \mathbf{E}\left[Y^4\right] = 3(\alpha^2 + \beta^2)^2\sigma^4 \\ \mathbf{E}\left[X^2Y^2\right] = \mathbf{E}\left[n_C^2(\alpha n_C + \beta n_S)^2\right] = \left(3\alpha^2 + \beta^2\right)\sigma^4 \end{cases}. \tag{A.10}$$

Therefore, the second term of (A.8) is given by

$$\mathbf{E}\left\{(X^2 + Y^2)^2\right\} = \left[3 + 2\left(3\alpha^2 + \beta^2\right) + 3(\alpha^2 + \beta^2)^2\right]\sigma^4. \tag{A.11}$$

$(U^2 + V^2)$ and $(Y^2 + X^2)$ are independent random variables. The third term of (A.8) is then obtained

$$\mathbf{E}\left[(U^2 + V^2) \cdot (X^2 + Y^2)\right] = \mathbf{E}\left[(U^2 + V^2)\right] \cdot \mathbf{E}\left[(X^2 + Y^2)\right] $$
$$= \frac{\sigma^2}{2}\left(1 + \alpha^2 + \beta^2\right)^2. \tag{A.12}$$

Due to the independence property between the variables (U, V) and (X, Y), the last term of (A.8) can be reformulated as

$$\mathbf{E}\left[(UX + VY)^2\right] = \mathbf{E}\left[U^2\right]\mathbf{E}\left[X^2\right] + 2\mathbf{E}\left[UV\right] \cdot \mathbf{E}\left[XY\right]$$
$$+ \mathbf{E}\left[V^2\right] \cdot \mathbf{E}\left[Y^2\right]. \tag{A.13}$$

The last term is expressed as

$$\mathbf{E}\left[(UX + VY)^2\right] = \left(\alpha^2 + \frac{1 + (\alpha^2 + \beta^2)^2}{2}\right) \cdot \sigma^2. \tag{A.14}$$

From (A.9), (A.11), (A.12) and (A.14), the variance of $|r|^2$ is finally derived (as in Eq. (8))

$$\mathbf{Var}\left(|r|^2\right) = \alpha^2\beta^2 + 2\left(1 + 2\alpha^2 + \left(\alpha^2 + \beta^2\right)^2\right) \cdot \left(1 + \alpha^2\right) \cdot \sigma^2. \tag{A.15}$$

Appendix B

If $\phi_0 = \arg\max_{\phi_{var}}\left(D_{(wo)}\left(\phi_{var}\right)\right)$ or $\tan\phi_0 = -\sin\phi_{mis}$, we evaluate the first derivative of $D(\phi)$ at $\phi = \phi_0$. To do that, the expression of D in Eq. (9) is represented as follows

$$D = \frac{Z\left(1 + \alpha^2 + \beta^2\right)^2}{\alpha^2\beta^2 - 2S\beta^2 + S(1 + \alpha^2 + \beta^2)^2} = \frac{Z}{S + \frac{\beta^2\left(\alpha^2 - 2S\right)}{(1+\alpha^2+\beta^2)^2}}. \tag{B.1}$$

where $Z = (1/2 + \sigma^2)^2$ and $S = 2\sigma^2(1 + \sigma^2)$. If we call $F_S\left(\phi\right) = \frac{\beta^2\left(\alpha^2 - 2S\right)}{(1+\alpha^2+\beta^2)^2}$, Eq. (B.1) can be re-written by

$$D = \frac{Z}{S + F_S\left(\phi\right)}. \tag{B.2}$$

By inspecting Eq. (B.2), it can be observed that the extremum of D corresponds to the extremum of $F_S(\phi)$. Instead of evaluating the first derivative of D at $\phi = \phi_0$, we can equivalently investigate the first derivative of $F_S(\phi)$ at $\phi = \phi_0$. In order to simplify the expression, the following variables and its corresponding derivative at $\phi = \phi_0$ are established

$$\begin{cases} u = \alpha^2, & v = \beta^2 \\ u_0 = \alpha^2\big|_{\phi=\phi_0} = 0, & v_0 = \beta^2\big|_{\phi=\phi_0} \\ u_0' = \left(\frac{d\left(\alpha^2\right)}{d\phi}\right)\Big|_{\phi=\phi_0} = 0, & v_0' = \left(\frac{d\left(\beta^2\right)}{d\phi}\right)\Big|_{\phi=\phi_0} \end{cases}. \tag{B.3}$$

The expression of $F_S(\phi)$ is now given by

$$F_S\left(\phi\right) = \frac{v\left(u - 2S\right)}{\left(1 + u + v\right)^2} \tag{B.4}$$

and its first derivative at $\phi = \phi_0$ can be established

$$\frac{d\left(F_S\left(\phi\right)\right)}{d\phi}\bigg|_{\phi=\phi_0} = \frac{v_0'\left(u_0 - 2S\right) + v_0\left(u_0' - 2S\right)}{\left(1 + u_0 + v_0\right)^2} - \frac{2v_0\left(u_0 - 2S\right)}{\left(1 + u_0 + v_0\right)^3} \tag{B.5}$$

or equivalently,

$$\frac{d\left(F_S\left(\phi\right)\right)}{d\phi}\bigg|_{\phi=\phi_0} = \frac{2S \cdot K}{\left(1 + v_0\right)^2}, \tag{B.6}$$

in which K is calculated by

$$K = \frac{2v_0}{1 + v_0} - \left(v_0 + v_0'\right). \tag{B.7}$$

Due to the fact that $\tan\phi_0 = -\sin\phi_{mis}$ and from the definition of β in Eq. (6), the values of v_0 and v_0' can be deduced as follows

$$\begin{cases} v_0 = \frac{\cos^2\phi_{mis}}{1+\sin^2\phi_{mis}} \\ v_0' = \frac{2\cos^2\phi_{mis}\sin\phi_{mis}}{1+\sin^2\phi_{mis}} \end{cases}. \tag{B.8}$$

Substituting (B.8) into (B.7), K can be obtained as

$$K = \frac{\cos^2\phi_{mis}\sin\phi_{mis}\left(\sin\phi_{mis} - 2\right)}{1 + \sin^2\phi_{mis}}. \tag{B.9}$$

From (B.6) and (B.9), it can be concluded that K is different from 0 and hence the first derivative of $F_S(\phi)$ at $\phi = \phi_0$ is also not equal to 0 whenever $S \neq 0$. As a consequence, the first derivative of $D(\phi)$ at $\phi = \phi_0$ differs from 0, so the dependence of the maximum value of D on the SNR of the received samples is confirmed.

References

[1] Raybon, G., Adamiecki, A., Winzer, P. J., Randel, S., Salamanca, L., Konczykowska, A., Jorge, F., Dupuy, J.-Y., Buhl, L. L., Chandrashekhar, S., Xie, C., Draving, S., Grove, M., Rush, K., and Urbanke, R.: High symbol rate coherent optical transmission systems: 80 and 107 Gbaud. J. Lightw Technol. 32, 824-831 (2014).

[2] Ip, E., Lau, A. P. T., Barros, D. J. F., and Kahn, J. M.: Coherent detection in optical fiber systems. Opt. Express 16, 753-791 (2008).

[3] Valkama, M., Renfors, M., and Koivunen, V.: Advanced methods for I/Q imbalance compensation in communication receivers. IEEE Trans. Signal Process. 49, 2335-2344 (2001).

[4] Liu, X.: Receiver sensitivity improvement in optical DQPSK and DQPSK/ASK through data-aided multi-symbol phase estimation. Proc. ECOC, p. Th.4.4.5 (2006).

[5] Savory, S. J.: Digital filters for coherent optical receivers. Opt. Express 16, 804-817 (2008).

[6] Ip, E., and Kahn, J. M.: Compensation of dispersion and nonlinear impairments using digital back propagation. J. Lightw. Technol. 26, 3416-3425 (2008).

[7] Anttila, L., Valkama, M., and Renfors, M.: Circularity-based I/Q imbalance compensation in wideband direct-conversion receivers. IEEE Trans. Veh. Technol. 57, 2099-2113 (2008).

[8] Schenk, T. C. W., Smulders, P. F. M., and Fledderus, E. R.: Estimation and compensation of frequency selective TX/RX IQ imbalance in MIMO OFDM systems. Proc. IEEE Int. Conf. Commun., pp. 251-256 (2006).

[9] Liu, C.-H.: Joint Tx and Rx IQ imbalance compensation of OFDM transceiver in mesh network. Proc. Globel Telecom. Conf., pp. 704-708 (2008).

[10] Chung, W.: Transmitter IQ mismatch compensation in coherent optical OFDM systems using pilot signals. Opt. Express 1, 21308-21314 (2010).

[11] Ma, X., Li, K., and Bai, Y.: Novel training symbol structure for transmitter IQ mismatch compensation for coherent optical OFDM. IEEE Photon. Technol. Lett. 25, 2047-2049 (2013).

[12] Cao, S., Yu, C., and Kam, P. Y.: Decision-aided joint compensation of transmitter IQ mismatch and phase noise for coherent optical OFDM. IEEE Photon. Technol. Lett. 24, 1066-1068 (2012).

[13] Fatadin, I., Savory, S. J., and Ives, D.: Compensation of quadrature imbalance in an optical QPSK coherent receiver. IEEE Photon. Technol. Lett. 20, 1733-1735 (2008).

[14] Chang, S. H., Chung, H. S., and Kim, K.: Impact of quadrature imbalance in optical coherent QPSK receiver. IEEE Photon. Technol. Lett. 21, 709-711 (2009).

[15] Petrou, C. S., Vgenis, A., Roudas, I., and Raptis, L.: Quadrature imbalance compensation for PDM QPSK coherent optical systems. IEEE Photon. Technol. Lett. 21, 1876-1878 (2009).

[16] Qiao, Y., Xu, Y., Li, L., and Ji, Y.: Quadrature imbalance compensation algorithm based on statistical properties of signals in CO-QPSK system. Chinese Opt. Lett. 10, 120601 (2012).

[17] Nguyen, T.-H., Gomez-Agis, F., Gay, M., Anet-Neto, L., Scalart, P., Peucheret, C., Joindot, M., Sentieys, O., Simon, J.-C., and Bramerie, L.: IQ imbalance compensation based on maximum SNR estimation in coherent QPSK systems. Proc. IEEE Int. Conf. Transparent Opt. Netw., p. Tu.C1.3 (2014).

[18] Razavi, B.: Design considerations for direct-conversion receivers. IEEE Trans. Circuits Syst. II, Analog Digit. Signal Process. 44, 428-435 (1997).

[19] Cardoso, J.-F., and Laheld, B. H.: Equivariant adaptive source separation. IEEE Trans. Signal Process. 44, 3017-3030 (1996).

[20] Vitthaladevuni, P. K., and Alouini, M.-S.: A recursive algorithm for the exact BER computation of generalized hierarchical QAM constellations. IEEE Trans. Inf. Theory 49, 297-307 (2003).

[21] Mizuochi, T.: Recent progress in forward error correction and its interplay with transmission impairments. IEEE J. Sel. Topics Quantum Electron. 12, 544-554 (2006).

[22] OIF: Implementation agreement for integrated dual polarization intradyne coherent receiver. IA# OIF-DPC-RX-01.2.

[23] Proakis, J.: Digital Communications, McGraw-Hill, 4th edition, Chap. 5 and Chap. 11 (2000).

[24] Viterbi, A. J., and Viterbi, A. M.: Nonlinear estimation of PSK-modulated carrier phase with application to burst digital transmission. IEEE Trans. Inf. Theory 29, 543-551 (1983).

[25] McKinley, M. D., Remley, K. A., Myslinski, M., Kenney, J. S., Schreurs, D., and Nauwelaers, B.: EVM calculation for broadband modulated signals. Proc. 64th ARFTG Conf. Dig., pp. 45-52 (2004).

[26] Fatadin, I., Ives, D., and Savory, S. J.: Laser linewidth tolerance for 16-QAM coherent optical systems using QPSK partitioning. IEEE Photon. Technol. Lett. 22, 631-634 (2010).

[27] Winzer, P. J., Gnauck, A. H., Doerr, C. R., Magarini, M., and Buhl, L. L.: Spectrally efficient long-haul optical networking using 112-Gb/s polarization-multiplexed 16-QAM. J. Lightw. Technol. 28, 547-556 (2010).

[28] Magnus, W., Oberhettinger, F., and Soni, R. P.: Formulas and Theorems for the Special Functions of Mathematical Physics, 3rd edition, Eds. Springer-Verlag (1966).